Molecular simulation of the phase behavior of noble gases using accurate two-body and three-body intermolecular potentials

Gianluca Marcelli and Richard J. Sadus[a)]
Computer Simulation and Physical Applications Group, School of Information Technology, Swinburne University of Technology, P.O. Box 218 Hawthorn, Victoria 3122, Australia

(Received 17 February 1999; accepted 28 April 1999)

Gibbs ensemble Monte Carlo simulations are reported for the vapor–liquid phase coexistence of argon, krypton, and xenon. The calculations employ accurate two-body potentials in addition to contributions from three-body dispersion interactions resulting from third-order triple-dipole, dipole–dipole–quadrupole, dipole–quadrupole–quadrupole, quadrupole–quadrupole–quadrupole, and fourth-order triple-dipole terms. It is shown that vapor–liquid equilibria are affected substantially by three-body interactions. The addition of three-body interactions results in good overall agreement of theory with experimental data. In particular, the subcritical liquid-phase densities are predicted accurately. © *1999 American Institute of Physics.*
[S0021-9606(99)50728-9]

I. INTRODUCTION

It is well established[1] that the physical properties of fluids are governed overwhelming by interactions involving pairs of molecules. However, it is also well-known[2–4] that three-body interactions can make a small but significant contribution to the energy of the liquid. Calculations of the configuration energy[2,4] of atoms indicate that three-body interactions make a contribution of typically 5%–10% to the overall energy. There is also evidence[3,4] to indicate that the contribution of three-body interactions for molecules is considerably higher. The influence this relatively small contribution has on the observed properties of the fluid is unclear. This uncertainty arises from a number of factors such as the adequacy of the two-body potential and the incomplete calculation of three-body interactions. Often, two-body potentials are used which do not truly reflect the contribution from two-body interactions but which effectively include contributions from other many-body interactions. Calculations of three-body interactions typically only consider contributions from the Axilrod–Teller[5] term. The Axilrod–Teller term only accounts for triple-dipole interactions whereas other three-body interactions arising from high multipoles are possible.[6,7] Furthermore, the effect of three-body repulsion is most commonly ignored.

The vapor–liquid phase transition represents an important property which is sensitive to intermolecular interactions. Gibbs ensemble Monte Carlo[8] simulations provide an effective means of relating the vapor–liquid transition to the underlying intermolecular interactions as described by a suitable intermolecular potential. Previous work[9–11] on the role of three-body interactions on the phase behavior of pure atomic systems has been restricted to the Axilrod–Teller term and the calculations have been confined exclusively to argon. In addition, calculations on the influence of three-body interactions on phase behavior of some theoretical binary mixtures are also available.[12,13] Sadus and Prausnitz[9] reported that the Axilrod–Teller term contributes typically 5% of the overall energy of the liquid phase of argon. Calculations for the vapor–liquid coexistence of argon by Anta *et al.*[10] and Sadus[11] using a combination of the Lennard-Jones and Axilrod–Teller potentials indicate that the inclusion of three-body interaction deteriorates the agreement between theory and experiment for the coexisting liquid phase densities. This failure can be attributed to the effective nature of the Lennard-Jones potential. Anta *et al.*[10] reported good results for vapor–liquid coexistence of argon using the Aziz–Slaman[14] potential in conjunction with the Axilrod–Teller term. Unlike the Lennard-Jones potential, the Aziz–Slaman potential is a genuine representation of the contribution of only two-body interactions.

The aim of this work is to investigate comprehensively the role of other multipole three-body dispersion terms in addition to the Axilrod–Teller term on the vapor–liquid transitions observed for argon, krypton, and xenon.

II. THEORY

A. Intermolecular potentials

Several accurate two-body potentials are available in the literature.[1] We have chosen to use the potentials proposed by Barker *et al.*[2,15–17] because of their well-known accuracy and the availability of intermolecular potential parameters for argon, krypton, and xenon. A recent review of intermolecular potential is available elsewhere.[18] The two-body interactions of argon are well represented by the Barker–Fisher–Watts (BFW) potential.[2] The BFW potential is a linear combination of the Barker–Pompe[15] (u_{BP}) and Bobetic–Barker[16] (u_{BB}) potentials,

$$u_2(r) = 0.75u_{\mathrm{BB}}(r) + 0.25u_{\mathrm{BP}}(r), \tag{1}$$

where the potentials of Barker–Pompe and Bobetic–Barker have the following form:

a)Author to whom correspondence should be addressed. Electronic mail: RSadus@swin.edu.au

TABLE I. Summary of the intermolecular potential parameters used in this work.

	Argon[a]		Krypton[b]	Xenon[c]
ν_{DDD}(a.u.)[d]	518.3		1572	5573
ν_{DDQ}(a.u.)[e]	687.5		2272	9448
ν_{DQQ}(a.u.)[e]	2687		9648	45770
ν_{QQQ}(a.u.)[e]	10639		41478	222049
ν_{DDD}(a.u.)[f]	−10570		−48465	−284560
ε/k(K)	142.095		201.9	281.0
σ(Å)	3.3605		3.573	3.890
R_m(Å)	3.7612		4.0067	4.3623
	Barker–Pompe	Bobetic–Barker		
α	12.5	12.5	12.5	12.5
α'			12.5	12.5
δ	0.01	0.01	0.01	0.01
A_0	0.2349	0.29214	0.23526	0.2402
A_1	−4.7735	−4.41458	−4.78686	−4.8169
A_2	−10.2194	−7.70182	−9.2	−10.9
A_3	−5.2905	−31.9293	−8.0	−25.0
A_4	0.0	−136.026	−30.0	−50.7
A_5	0.0	−151.0	−205.8	−200.0
P			−9.0	59.3
Q			68.67	71.1
C_6	1.0698	1.11976	1.0632	1.0544
C_8	0.1642	0.171551	0.1701	0.1660
C_{10}	0.0132	0.013748	0.0143	0.0323

[a]Two-body parameters from Ref. 2.
[b]Two-body parameters from Ref. 17.
[c]Two-body parameters from Ref. 17.
[d]From Ref. 20.
[e]From Ref. 22.
[f]From Ref. 21.

$$u_2(r)=\varepsilon\left[\sum_{i=0}^{5} A_i(x-1)^i \exp[\alpha(1-x)]-\sum_{j=0}^{2}\frac{C_{2j+6}}{\delta+x^{2j+6}}\right]. \tag{2}$$

In Eq. (2), $x=r/r_m$ where r_m is the intermolecular separation at which the potential has a minimum value and the other parameters are obtained by fitting the potential to experimental data for molecular beam scattering, second virial coefficients, and long-range interaction coefficients. The contribution from repulsion has an exponential-dependence on intermolecular separation and the contribution to dispersion of the C_6, C_8, and C_{10} coefficients are included. The only difference between the Barker–Pompe and Bobetic–Barker potentials is that a different set of parameters is used in each case. These parameters[2] are summarized in Table I.

The molecule-specific nature of the intermolecular potential is illustrated by attempts to use Eq. (2) for other noble gases such as krypton and xenon. Barker *et al.*[17] reported that modifications to Eq. (2) were required to obtain an optimal representation for these larger noble gases. For krypton and xenon, they determined a potential of the form:

$$u_2(r)=u_0(r)+u_1(r), \tag{3}$$

where $u_0(r)$ is identical to Eq. (2) and $u_1(r)$ is given by:

$$u_1(r)=\begin{cases}[P(x-1)^4+Q(x-1)^5\exp[\alpha'(1-x)] & x>1,\\ 0 & x\leqslant 1,\end{cases} \tag{4}$$

and α', P, and Q are additional parameters obtained by fitting data for differential scattering cross sections. In this work we have used Eq. (3) to predict the properties of krypton and xenon with the parameters[17] summarized in Table I.

Different types of interaction are possible depending on the distribution of multipole moments between the atoms. In principle, the dispersion or long-range nonadditive three-body interaction is the sum of these various combinations of multipole moments.[6] In this work, we have considered contributions from dipoles (D) and quadrupoles (Q) which are likely to make the most substantial effects on three-body dispersion:

$$u_{3BDisp}=u_{DDD}+u_{DDQ}+u_{DQQ}+u_{DDD4}+u_{QQQ}. \tag{5}$$

These terms are all third-order with the exception of the contribution of the fourth-order triple-dipole term (u_{DDD4}). The main contribution to attractive three-body interaction is the third-order triple-dipole term (u_{DDD}). The other terms collectively ($u_{DDQ}+u_{DQQ}+u_{QQQ}+u_{DDD4}$) are the higher multipole contributions.

The triple-dipole potential can be evaluated from the formula proposed by Axilrod and Teller[5]:

$$u_{DDD}(ijk)=\frac{\nu_{DDD}(ijk)(1+3\cos\theta_i\cos\theta_j\cos\theta_k)}{(r_{ij}r_{ik}r_{jk})^3}, \tag{6}$$

where $\nu_{DDD}(ijk)$ is the nonadditive coefficient, and the angles and intermolecular separations refer to a triangular configuration of atoms. A detailed derivation of Eq. (6) from third-order perturbation theory has been given by Axilrod.[19]

The contribution of the Axilrod–Teller potential can be either negative or positive depending on the orientation

adopted by the three atoms. The potential is positive for an acute triangular arrangement of atoms whereas it is negative for near linear geometries. The potential can be expected to make an overall repulsive contribution in a close-packed solid and in the liquid-phase. The r^{-3} terms indicate that the magnitude of the potential is very dependent on intermolecular separation. The major contribution to the potential will occur for configurations in which at least one pair of atoms is in close proximity to each other.

Bell[6] has derived the other multipolar nonadditive third-order potentials:

$$u_{\mathrm{DDQ}}(ijk)=\frac{3\nu_{\mathrm{DDQ}}(ijk)}{16r_{ij}^{3}(r_{jk}r_{ik})^{4}}\times[9\cos\theta_k-25\cos 3\theta_k+6\cos(\theta_i-\theta_j)(3+5\cos 2\theta_k)], \tag{7}$$

$$u_{\mathrm{DQQ}}(ijk)=\frac{15\nu_{\mathrm{DQQ}}(ijk)}{64r_{jk}^{5}(r_{ij}r_{ik})^{4}}\times\left[\begin{array}{l}3(\cos\theta_i+5\cos 3\theta_i)+20\cos(\theta_j-\theta_k)(1-3\cos 2\theta_i)\\ \quad+70\cos 2(\theta_j-\theta_k)\cos\theta_i\end{array}\right], \tag{8}$$

$$u_{\mathrm{QQQ}}(ijk)=\frac{15\nu_{\mathrm{QQQ}}(ijk)}{128(r_{ij}r_{ik}r_{jk})^{5}}\times\left[\begin{array}{l}-27+220\cos\theta_i\cos\theta_j\cos\theta_k+490\cos 2\theta_i\cos 2\theta_j\cos 2\theta_k\\ \quad+175[\cos 2(\theta_i-\theta_j)+\cos 2(\theta_j-\theta_k)+\cos 2(\theta_k-\theta_i)]\end{array}\right], \tag{9}$$

where Eqs. (7), (8), and (9) represent the effect of dipole–dipole–quadrupole, dipole–quadrupole–quadrupole, and quadrupole–quadrupole–quadrupole interactions, respectively. Formulas for the different ordering of the multipole moments on the three atoms (i.e., QDD, DQD, QDQ, and QQD) can be generated from Eqs. (8) and (9) by cyclic permutation of θ_i, θ_j, θ_k, and r_{ik}. The dipole–dipole–octupole term has also been evaluated by Doran and Zucker[7] but it is not considered in this work because of uncertainties in evaluating the DDO coefficient. The fourth-order triple-dipole term can be evaluated from[7]

$$u_{\mathrm{DDD4}}(ijk)=\frac{45\nu_{\mathrm{DDD4}}(ijk)}{64}\left[\frac{1+\cos^2\theta_i}{(r_{ik}r_{ij})^{6}}+\frac{1+\cos^2\theta_j}{(r_{ij}r_{jk})^{6}}+\frac{1+\cos^2\theta_k}{(r_{ik}r_{jk})^{6}}\right]. \tag{10}$$

The coefficients[20–22] for these three-body terms are summarized in Table I. Strategies for calculating multipole moments have been discussed recently.[22] Combining the contributions from two-body and three-body interactions yields an overall intermolecular potential for the fluid:

$$u(r)=u_2(r)+u_{\mathrm{3BDisp}}(r). \tag{11}$$

B. Simulation details

The NVT Gibbs ensemble[8] was implemented for a system of 500 atoms. The simulations were performed in cycles consisting typically of 500 attempted displacements, an attempted volume change and 500 interchange attempts. Typically, 1500 cycles were used for equilibration and a further 1500 cycles were used to accumulate ensemble averages. Periodic boundary conditions were applied. The two-body potentials were truncated at half the box length and appropriate long range correction terms were evaluated to recover the contribution to pressure, energy, and chemical potential of the full intermolecular potential.[23] Some care needs to be taken with the three-body potentials because the application of a periodic boundary can potentially destroy the position-invariance of three particles.[24] We examined the behavior of the three-body terms for many thousands of different orientations and intermolecular separations. All the three-body terms asymptote rapidly to zero with increasing intermolecular separation. For a system size of 500 or more atoms, we

TABLE II. Vapor–liquid coexistence properties of argon from molecular simulation using the two-body BFW potential [Eq. (1)]. The values in brackets represent the uncertainty of the last digit.

T^*	ρ_{L}^*	P_{L}^*	E_{L}^*	μ_{L}^*	ρ_{V}^*	P_{V}^*	E_{V}^*	μ_{V}^*
0.700	0.806(4)	−0.018(38)	−5.18(3)	−3.67	0.006(1)	0.004(1)	−0.06(2)	−3.70
0.750	0.781(3)	0.007(21)	−4.98(2)	−3.67	0.008(1)	0.006(1)	−0.08(3)	−3.68
0.825	0.741(4)	0.020(14)	−4.66(3)	−3.43	0.021(2)	0.015(2)	−0.19(3)	−3.39
0.850	0.727(5)	0.022(19)	−4.56(3)	−3.49	0.023(2)	0.017(3)	−0.21(3)	−3.42
0.875	0.711(5)	0.017(16)	−4.44(4)	−3.47	0.030(2)	0.022(3)	−0.26(3)	−3.36
0.900	0.696(5)	0.022(19)	−4.33(4)	−3.39	0.033(3)	0.025(3)	−0.29(3)	−3.38
0.925	0.678(3)	0.036(10)	−4.20(2)	−3.40	0.041(2)	0.031(3)	−0.35(3)	−3.32
0.950	0.661(10)	0.037(22)	−4.08(6)	−3.35	0.049(5)	0.037(7)	−0.41(4)	−3.30
0.975	0.644(6)	0.049(16)	−3.97(4)	−3.34	0.057(5)	0.042(6)	−0.47(4)	−3.28
1.000	0.622(7)	0.056(13)	−3.81(4)	−3.24	0.073(7)	0.051(12)	−0.59(6)	−3.23
1.025	0.597(8)	0.062(17)	−3.66(5)	−3.25	0.082(6)	0.058(11)	−0.64(6)	−3.23
1.050	0.574(9)	0.071(21)	−3.50(5)	−3.22	0.104(7)	0.069(13)	−0.82(6)	−3.18
1.075	0.540(12)	0.080(27)	−3.31(7)	−3.20	0.112(10)	0.075(19)	−0.86(8)	−3.20

TABLE III. Vapor–liquid coexistence properties of argon from molecular simulation using the two-body BFW potential [Eq. (1)]+three-body (DDD+DDQ +DQQ+DDD4) intermolecular potentiais. The values in brackets represent the uncertainty of the last digit.

	T^*								
	0.750	0.825	0.850	0.875	0.900	0.925	0.950	0.975	1.00
ρ_L^*	0.742(5)	0.685(8)	0.671(10)	0.658(10)	0.639(11)	0.613(11)	0.600(10)	0.564(11)	0.513(30)
$P_{L\ tot}^*$	0.044(89)	0.017(38)	0.020(50)	0.028(41)	0.033(52)	0.035(41)	0.049(36)	0.045(39)	0.052(100)
$P_{L\ 2body}^*$	−0.914(77)	−0.854(21)	−0.825(30)	−0.809(21)	−0.788(30)	−0.743(20)	−0.718(17)	−0.673(19)	−0.591(51)
$P_{L\ DDD}^*$	0.375(8)	0.271(9)	0.250(10)	0.235(8)	0.218(9)	0.190(9)	0.175(7)	0.149(7)	0.117(15)
$P_{L\ DDQ}^*$	0.125(3)	0.090(3)	0.083(3)	0.078(3)	0.072(3)	0.062(3)	0.057(2)	0.049(3)	0.038(5)
$P_{L\ DQQ}^*$	0.0254(7)	0.0186(7)	0.0170(7)	0.0159(6)	0.0147(6)	0.0127(7)	0.0117(6)	0.0099(6)	0.0076(11)
$P_{L\ QQQ}^*$	0.0023(1)	0.0017(1)	0.0015(1)	0.0014(1)	0.0013(1)	0.0011(1)	0.0010(1)	0.0009(1)	0.0007(1)
$P_{L\ DDD4}^*$	−0.124(3)	−0.074(2)	−0.068(2)	−0.063(2)	−0.058(1)	−0.052(2)	−0.046(1)	−0.040(1)	−0.033(3)
$E_{L\ tot}^*$	−4.53(3)	−4.13(6)	−4.01(7)	−3.97(5)	−3.89(7)	−3.68(6)	−3.57(6)	−3.39(6)	−3.09(16)
$E_{L\ 2body}^*$	−4.73(3)	−4.33(6)	−4.16(6)	−4.06(7)	−3.99(6)	−3.83(7)	−3.71(6)	−3.49(6)	−3.19(16)
$E_{L\ DDD}^*$	0.169(3)	0.132(3)	0.125(3)	0.119(3)	0.113(3)	0.103(3)	0.097(2)	0.088(3)	0.076(6)
$E_{L\ DDQ}^*$	0.046(1)	0.036(1)	0.034(1)	0.032(1)	0.031(1)	0.028(1)	0.026(1)	0.023(1)	0.020(2)
$E_{L\ DQQ}^*$	0.0079(2)	0.0063(2)	0.0059(2)	0.0056(1)	0.0053(1)	0.0048(2)	0.0045(1)	0.0040(2)	0.0034(3)
$E_{L\ QQQ}^*$	0.00061(2)	0.00049(1)	0.00046(1)	0.00043(1)	0.00041(1)	0.00037(1)	0.00035(1)	0.00031(1)	0.00026(2)
$E_{L\ DDD4}^*$	−0.0419(10)	−0.0268(4)	−0.0256(4)	−0.0240(5)	−0.0227(4)	−0.0212(5)	−0.0192(4)	−0.0178(5)	−0.0161(7)
μ_L^*	−3.47	−3.48	−3.53	−3.40	−3.35	−3.36	−3.29	−3.26	−3.28
ρ_V^*	0.0095(17)	0.0174(15)	0.0218(18)	0.0295(37)	0.0350(48)	0.0401(38)	0.0536(56)	0.0605(52)	0.0655(32)
$P_{V\ tot}^*$	0.0067(16)	0.0128(17)	0.0162(21)	0.0216(46)	0.0259(64)	0.0301(51)	0.0388(83)	0.0440(83)	0.0490(56)
$P_{V\ 2body}^*$	−0.0005(4)	−0.0016(4)	−0.0024(5)	−0.0043(13)	−0.0057(20)	−0.0071(15)	−0.0126(28)	−0.0155(31)	−0.0172(23)
$P_{V\ DDD}^* 10^{-3}$	0.0005(22)	0.0212(156)	0.0432(198)	0.0846(533)	0.1350(726)	0.1911(609)	0.442(116)	0.567(145)	0.700(138)
$P_{V\ DDQ}^* 10^{-4}$	0.001(4)	0.070(65)	0.128(66)	0.249(172)	0.406(217)	0.572(188)	1.313(341)	1.67(418)	2.067(428)
$P_{V\ DQQ}^* 10^{-5}$	0.001(6)	0.148(167)	0.239(142)	0.468(364)	0.775(418)	1.092(374)	2.486(636)	3.135(773)	3.896(864)
$P_{V\ QQQ}^* 10^{-6}$	0.001(4)	0.135(170)	0.198(132)	0.390(336)	0.659(362)	0.931(327)	2.106(532)	2.648(646)	3.307(779)
$P_{V\ DDD4}^* 10^{-4}$	−0.0016(25)	−0.048(28)	−0.111(55)	−0.234(135)	−0.385(220)	−0.530(168)	−1.249(330)	−1.628(408)	−2.015(371)
$E_{V\ tot}^*$	−0.07(2)	−0.15(3)	−0.20(3)	−0.26(5)	−0.30(5)	−0.34(3)	−0.45(4)	−0.49(5)	−0.52(3)
$E_{V\ 2body}^*$	−0.07(2)	−0.15(3)	−0.20(3)	−0.26(5)	−0.30(5)	−0.34(3)	−0.46(4)	−0.49(5)	−0.52(3)
$E_{V\ DDD}^* 10^{-3}$	0.02(7)	0.39(28)	0.64(28)	0.87(45)	1.21(49)	1.55(37)	2.65(46)	2.98(55)	3.47(60)
$E_{V\ DDQ}^* 10^{-3}$	0.003(10)	0.11(9)	0.16(8)	0.21(12)	0.30(12)	0.38(9)	0.65(11)	0.72(13)	0.84(16)
$E_{V\ DQQ}^* 10^{-4}$	0.002(12)	0.19(20)	0.25(15)	0.33(23)	0.48(21)	0.62(16)	1.04(17)	1.14(20)	1.34(27)
$E_{V\ QQQ}^* 10^{-5}$	0.001(7)	0.15(18)	0.18(12)	0.24(18)	0.35(16)	0.46(13)	0.76(13)	0.84(15)	0.98(22)
$E_{V\ DDD4}^* 10^{-3}$	−0.004(6)	−0.066(36)	−0.124(59)	−0.182(83)	−0.259(111)	−0.322(75)	−0.563(102)	−0.642(115)	−0.750(119)
μ_V^*	−3.57	−3.51	−3.46	−3.36	−3.34	−3.34	−3.25	−3.25	−3.26

found truncating the three-body potentials at intermolecular separations greater than a quarter of the length of the simulation box to be an excellent approximation to the full potential that also avoided the problem of three-body invariance to periodic boundary conditions. The three-body simulations commonly require 20 and 12 CPU h on the Fujitsu VP300 and NEC SX-4/32 supercomputers, respectively.

III. RESULTS AND DISCUSSION

The results of Gibbs ensemble simulations for the vapor–liquid properties of argon, krypton, and xenon are reported in Tables II–VII. The remaining stable noble gases, helium and neon, were not considered because of uncertainties arising from quantum effects. Some molecular dynamics

TABLE IV. Vapor–liquid coexistence properties of krypton from molecular simulation using the two-body Barker *et al.* potential [Eq. (3)]. The values in brackets represent the uncertainty of the last digit.

T^*	ρ_L^*	P_L^*	E_L^*	μ_L^*	ρ_V^*	P_V^*	E_V^*	μ_V^*
0.700	0.800(4)	−0.002(33)	−5.05(3)	−3.58	0.007(2)	0.005(1)	−0.07(3)	−3.55
0.750	0.774(3)	0.001(21)	−4.84(3)	−3.55	0.010(1)	0.007(1)	−0.09(2)	−3.53
0.825	0.735(5)	0.020(19)	−4.53(4)	−3.39	0.024(2)	0.017(2)	−0.21(2)	−3.31
0.850	0.718(4)	0.013(12)	−4.41(3)	−3.35	0.026(2)	0.019(2)	−0.22(3)	−3.34
0.875	0.700(5)	0.020(15)	−4.28(4)	−3.33	0.031(4)	0.023(4)	−0.27(4)	−3.32
0.900	0.687(5)	0.034(12)	−4.18(3)	−3.28	0.041(4)	0.030(4)	−0.36(4)	−3.24
0.925	0.666(7)	0.036(16)	−4.04(4)	−3.26	0.048(7)	0.034(10)	−0.41(7)	−3.23
0.950	0.647(3)	0.044(13)	−3.91(2)	−3.23	0.059(3)	0.041(5)	−0.48(3)	−3.18
0.975	0.624(9)	0.048(18)	−3.76(6)	−3.19	0.067(5)	0.047(7)	−0.54(4)	−3.18
1.000	0.609(6)	0.065(14)	−3.66(3)	−3.16	0.087(4)	0.059(7)	−0.68(5)	−3.12
1.025	0.573(17)	0.073(26)	−3.44(9)	−3.16	0.098(12)	0.065(20)	−0.75(8)	−3.13
1.050	0.548(18)	0.084(31)	−3.28(9)	−3.12	0.131(18)	0.080(33)	−0.98(14)	−3.09
1.065	0.530(23)	0.094(46)	−3.18(12)	−3.11	0.141(16)	0.082(33)	−1.05(11)	−3.08

TABLE V. Vapor–liquid coexistence properties of krypton from molecular simulation using the two-body Barker *et al.* [Eq. (3)]+three-body (DDD+DDQ +DQQ+DDD4) intermolecular potentials. The values in brackets represent the uncertainty of the last digit.

	T^*							
	0.750	0.825	0.850	0.875	0.900	0.925	0.950	0.975
ρ_L^*	0.712(6)	0.671(9)	0.642(9)	0.631(8)	0.616(7)	0.585(14)	0.528(23)	0.509(23)
$P_{L\ tot}^*$	0.051(75)	0.026(45)	0.028(35)	0.036(39)	0.040(26)	0.048(48)	0.045(77)	0.066(71)
$P_{L\ 2body}^*$	−0.899(46)	−0.848(23)	−0.807(15)	−0.784(21)	−0.758(12)	−0.703(20)	−0.616(40)	−0.573(34)
$P_{L\ DDD}^*$	0.390(25)	0.306(12)	0.273(9)	0.255(11)	0.233(7)	0.202(13)	0.157(13)	0.138(12)
$P_{L\ DDQ}^*$	0.127(9)	0.098(4)	0.088(3)	0.082(4)	0.074(2)	0.064(4)	0.049(4)	0.043(4)
$P_{L\ DQQ}^*$	0.0253(18)	0.0194(9)	0.0172(7)	0.0160(8)	0.0146(5)	0.0125(9)	0.0095(9)	0.0084(8)
$P_{L\ QQQ}^*$	0.0022(2)	0.0017(1)	0.0015(1)	0.0014(1)	0.00125(5)	0.0011(1)	0.0008(1)	0.0007(1)
$P_{L\ DDD4}^*$	−0.135(11)	−0.105(3)	−0.096(2)	−0.087(4)	−0.079(2)	−0.071(3)	−0.056(3)	−0.049(4)
$E_{L\ tot}^*$	−4.28(3)	−3.98(6)	−3.83(5)	−3.72(5)	−3.59(4)	−3.43(8)	−3.13(10)	−3.00(11)
$E_{L\ 2body}^*$	−4.49(4)	−4.08(7)	−3.97(5)	−3.88(6)	−3.75(4)	−3.55(8)	−3.23(10)	−3.10(11)
$E_{L\ DDD}^*$	0.183(11)	0.152(4)	0.141(3)	0.134(4)	0.126(2)	0.115(5)	0.098(4)	0.090(5)
$E_{L\ DDQ}^*$	0.049(3)	0.040(1)	0.037(1)	0.035(1)	0.033(1)	0.030(1)	0.025(1)	0.023(1)
$E_{L\ DQQ}^*$	0.0082(6)	0.0067(2)	0.0062(2)	0.0058(2)	0.0055(1)	0.0049(2)	0.0041(2)	0.0038(2)
$E_{L\ QQQ}^*$	0.00061(4)	0.00050(2)	0.00046(1)	0.00043(2)	0.00041(1)	0.00036(2)	0.00030(2)	0.00028(2)
$E_{L\ DDD4}^*$	−0.047(4)	−0.039(1)	−0.0372(5)	−0.035(1)	−0.032(1)	−0.030(1)	−0.027(1)	−0.024(1)
μ_L^*	−3.62	−3.37	−3.38	−3.24	−3.15	−3.24	−3.20	−3.17
ρ_V^*	0.0105(12)	0.0203(15)	0.0246(20)	0.0348(37)	0.0429(17)	0.0477(31)	0.0578(33)	0.0737(61)
$P_{V\ tot}^*$	0.0074(12)	0.0148(18)	0.0183(25)	0.0253(50)	0.0316(25)	0.0350(45)	0.0409(46)	0.0507(104)
$P_{V\ 2body}^*$	−0.0005(3)	−0.0020(6)	−0.0027(8)	−0.0054(17)	−0.0073(9)	−0.0095(16)	−0.0146(14)	−0.0224(42)
$P_{V\ DDD}^* 10^{-3}$	0.006(6)	0.0374(148)	0.0653(232)	0.171(77)	0.269(44)	0.338(67)	0.652(117)	1.20(29)
$P_{V\ DDQ}^* 10^{-4}$	0.018(24)	0.111(42)	0.185(75)	0.497(228)	0.795(142)	0.971(183)	1.86(36)	3.44(85)
$P_{V\ DQQ}^* 10^{-5}$	0.029(53)	0.205(81)	0.327(153)	0.908(423)	1.47(29)	1.74(32)	3.33(69)	6.22(1.58)
$P_{V\ QQQ}^* 10^{-6}$	0.024(50)	0.168(71)	0.257(131)	0.738(345)	1.21(26)	1.40(25)	2.67(58)	5.05(1.31)
$P_{V\ DDD4}^* 10^{-4}$	−0.036(24)	−0.127(34)	−0.225(58)	−0.601(255)	−0.978(156)	−1.27(26)	−2.38(40)	−4.40(1.08)
$E_{V\ tot}^*$	−0.09(2)	−0.18(3)	−0.21(2)	−0.29(4)	−0.36(2)	−0.38(3)	−0.47(3)	−0.58(6)
$E_{V\ 2body}^*$	−0.09(2)	−0.18(3)	−0.21(2)	−0.30(4)	−0.36(2)	−0.39(3)	−0.47(3)	−0.58(6)
$E_{V\ DDD}^* 10^{-3}$	0.18(17)	0.59(22)	0.86(24)	1.56(55)	2.08(30)	2.31(33)	3.64(46)	5.27(90)
$E_{V\ DDQ}^* 10^{-3}$	0.04(5)	0.14(5)	0.20(6)	0.37(14)	0.50(8)	0.54(7)	0.85(12)	1.24(22)
$E_{V\ DQQ}^* 10^{-4}$	0.05(10)	0.23(9)	0.30(11)	0.58(23)	0.79(14)	0.82(11)	1.28(20)	1.89(35)
$E_{V\ QQQ}^* 10^{-5}$	0.04(8)	0.16(7)	0.20(8)	0.41(16)	0.56(11)	0.57(8)	0.89(15)	1.33(26)
$E_{V\ DDD4}^* 10^{-3}$	−0.082(50)	−0.149(38)	−0.222(48)	−0.411(138)	−0.567(77)	−0.649(94)	−0.996(113)	−1.45(25)
μ_V^*	−3.52	−3.40	−3.37	−3.25	−3.20	−3.21	−3.19	−3.13

studies and *ab initio* calculations for helium and neon have been reported recently.[25–27] The normal convention was adopted for the reduced density ($\rho^*=\rho\sigma^3$), temperature ($T^*=kT/\varepsilon$), energy ($E^*=E/\varepsilon$), pressure ($P^*=P\sigma^3/\varepsilon$) and chemical potential ($\mu^*=\mu/\varepsilon$). The chemical potential was determined from the equation proposed by Smit *et al.*[28] The uncertainties in the ensemble averages for density, temperature, energy, and pressure reported in Tables II–VII were calculated by dividing the post-equilibrium results into ten sections. The estimated errors represent the standard deviations of the section averages. An error estimate for the chemical potential cannot be estimated in this way because it is the average of the entire post-equilibrium simulation. A comparison of simulation results with experiment is given in

TABLE VI. Vapor–liquid coexistence properties of xenon from molecular simulation using the two-body Barker *et al.* potential [Eq. (3)]. The values in brackets represent the uncertainty of the last digit.

T^*	ρ_L^*	P_L^*	E_L^*	μ_L^*	ρ_V^*	P_V^*	E_V^*	μ_V^*
0.700	0.801(5)	−0.010(36)	−5.07(3)	−3.72	0.006(1)	0.004(1)	−0.06(2)	−3.63
0.750	0.777(4)	−0.005(21)	−4.88(3)	−3.43	0.011(2)	0.008(1)	−0.10(2)	−3.49
0.825	0.733(4)	0.005(15)	−4.54(2)	−3.32	0.022(3)	0.016(3)	−0.20(4)	−3.35
0.850	0.715(6)	0.021(20)	−4.41(4)	−3.42	0.027(3)	0.020(3)	−0.24(3)	−3.32
0.875	0.701(3)	0.027(20)	−4.31(2)	−3.37	0.032(3)	0.023(4)	−0.28(3)	−3.30
0.900	0.682(4)	0.026(19)	−4.17(3)	−3.34	0.037(3)	0.027(4)	−0.32(3)	−3.29
0.925	0.664(8)	0.031(16)	−4.05(5)	−3.28	0.047(6)	0.034(7)	−0.39(4)	−3.24
0.950	0.644(9)	0.038(22)	−3.91(6)	−3.25	0.055(3)	0.040(4)	−0.46(3)	−3.22
0.975	0.623(9)	0.045(21)	−3.77(6)	−3.20	0.068(6)	0.048(10)	−0.55(7)	−3.18
1.000	0.605(9)	0.063(23)	−3.65(6)	−3.18	0.082(6)	0.056(10)	−0.65(4)	−3.15
1.025	0.583(11)	0.072(19)	−3.51(7)	−3.15	0.099(9)	0.066(15)	−0.77(6)	−3.12
1.050	0.549(14)	0.083(27)	−3.30(8)	−3.15	0.123(10)	0.077(19)	−0.94(8)	−3.10
1.075	0.501(88)	0.103(183)	−3.02(48)	−3.10	0.160(17)	0.088(34)	−1.18(12)	−3.07

TABLE VII. Vapor–liquid coexistence properties of xenon from molecular simulation using the two-body Barker *et al.* [Eq. (3)]+three-body (DDD+DDQ +DQQ+DDD4) intermolecular potentials. The values in brackets represent the uncertainty of the last digit.

	T^*							
	0.750	0.825	0.850	0.875	0.900	0.925	0.950	0.975
ρ^*_L	0.706(6)	0.671(9)	0.634(12)	0.617(15)	0.599(11)	0.578(13)	0.517(23)	0.511(26)
$P^*_{L\,tot}$	0.009(38)	0.024(53)	0.010(46)	0.030(64)	0.031(44)	0.059(61)	0.039(79)	0.060(89)
$P^*_{L\,2body}$	−0.947(26)	−0.875(29)	−0.828(20)	−0.779(31)	−0.751(21)	−0.696(34)	−0.611(39)	−0.596(42)
$P^*_{L\,DDD}$	0.444(9)	0.364(15)	0.314(14)	0.288(18)	0.260(13)	0.235(14)	0.178(16)	0.169(20)
$P^*_{L\,DDQ}$	0.140(3)	0.114(5)	0.098(5)	0.090(6)	0.081(4)	0.073(5)	0.054(5)	0.052(6)
$P^*_{L\,DQQ}$	0.0268(6)	0.0216(10)	0.0184(9)	0.0168(12)	0.0150(8)	0.0136(9)	0.0100(10)	0.0095(13)
$P^*_{L\,QQQ}$	0.0022(1)	0.0018(1)	0.0015(1)	0.0014(1)	0.0012(1)	0.0011(1)	0.0008(1)	0.0008(1)
$P^*_{L\,DDD4}$	−0.191(5)	−0.157(5)	−0.139(4)	−0.128(5)	−0.114(5)	−0.102(5)	−0.082(5)	−0.074(6)
$E^*_{L\,tot}$	−4.21(4)	−3.96(6)	−3.78(6)	−3.63(8)	−3.52(6)	−3.40(8)	−3.07(10)	−3.02(13)
$E^*_{L\,2body}$	−4.48(4)	−4.10(7)	−3.93(7)	−3.80(9)	−3.64(7)	−3.53(8)	−3.17(11)	−3.13(14)
$E^*_{L\,DDD}$	0.209(3)	0.181(5)	0.165(5)	0.155(6)	0.145(5)	0.135(5)	0.114(5)	0.109(7)
$E^*_{L\,DDQ}$	0.054(1)	0.047(1)	0.042(1)	0.040(2)	0.037(1)	0.034(1)	0.028(2)	0.027(2)
$E^*_{L\,DQQ}$	0.0087(2)	0.0075(3)	0.0067(2)	0.0063(3)	0.0058(2)	0.0054(2)	0.0044(3)	0.0043(4)
$E^*_{L\,QQQ}$	0.00062(1)	0.00053(2)	0.00047(2)	0.00044(2)	0.00041(2)	0.00038(2)	0.00031(2)	0.00030(3)
$E^*_{L\,DDD4}$	−0.067(1)	−0.059(1)	−0.055(1)	−0.052(1)	−0.048(2)	−0.044(2)	−0.039(1)	−0.036(1)
μ^*_L	−3.41	−3.28	−3.33	−3.30	−3.22	−3.20	−3.18	−3.15
ρ^*_V	0.0109(17)	0.0227(27)	0.0245(27)	0.0313(36)	0.0414(45)	0.0513(67)	0.0566(46)	0.0746(33)
$P^*_{V\,tot}$	0.0075(16)	0.0163(31)	0.0180(31)	0.0229(43)	0.0301(57)	0.0366(97)	0.0419(66)	0.0514(54)
$P^*_{V\,2body}$	−0.0006(3)	−0.0025(8)	−0.0030(8)	−0.0046(11)	−0.0075(15)	−0.0113(34)	−0.0125(21)	−0.0227(20)
$P^*_{V\,DDD}\,10^{-3}$	0.0050(75)	0.0686(472)	0.0838(364)	0.148(62)	0.311(116)	0.542(177)	0.717(105)	1.546(217)
$P^*_{V\,DDQ}\,10^{-4}$	0.009(24)	0.198(151)	0.233(111)	0.411(175)	0.883(345)	1.518(472)	2.031(296)	4.365(650)
$P^*_{V\,DQQ}\,10^{-5}$	0.002(50)	0.357(299)	0.400(216)	0.706(307)	1.559(640)	2.642(798)	3.573(524)	7.67(121)
$P^*_{V\,QQQ}\,10^{-6}$	−0.006(41)	0.282(251)	0.302(184)	0.534(241)	1.213(519)	2.039(613)	2.789(412)	5.969(982)
$P^*_{V\,DDD4}\,10^{-4}$	−0.0317(242)	−0.299(163)	−0.367(136)	−0.637(291)	−1.416(559)	−2.475(791)	−3.293(514)	−7.17(102)
$E^*_{V\,tot}$	−0.11(2)	−0.21(3)	−0.21(3)	−0.27(4)	−0.34(5)	−0.42(6)	−0.45(3)	−0.59(3)
$E^*_{V\,2body}$	−0.11(2)	−0.21(4)	−0.21(3)	−0.27(4)	−0.35(5)	−0.42(6)	−0.45(3)	−0.60(3)
$E^*_{V\,DDD}\,10^{-3}$	0.15(25)	0.94(57)	1.08(45)	1.50(49)	2.39(66)	3.38(73)	4.12(34)	6.67(68)
$E^*_{V\,DDQ}\,10^{-3}$	0.02(7)	0.22(15)	0.25(11)	0.34(12)	0.56(17)	0.78(16)	0.95(8)	1.54(17)
$E^*_{V\,DQQ}\,10^{-4}$	−0.01(13)	0.34(25)	0.36(19)	0.49(17)	0.83(27)	1.15(23)	1.42(13)	2.29(27)
$E^*_{V\,QQQ}\,10^{-5}$	−0.02(9)	0.23(18)	0.24(14)	0.32(12)	0.56(19)	0.77(16)	0.96(9)	1.55(19)
$E^*_{V\,DDD4}\,10^{-3}$	−0.078(65)	−0.307(144)	−0.356(120)	−0.479(168)	−0.815(237)	−1.158(234)	−1.415(127)	−2.316(241)
μ^*_V	−3.50	−3.34	−3.38	−3.32	−3.23	−3.19	−3.20	−3.13

Figs. 1, 3, and 4. The relative contribution to energy of the various three-body interactions for the liquid-phase of argon is illustrated in Fig. 2.

The coexistence properties obtained from argon using the BFW potential are summarized in Table II and the BFW +three-body calculations are reported in Table III. In Fig. 1, experimental data for the vapor–liquid phase envelope of argon are compared with simulation results obtained in this work and data reported by Anta *et al.*[10] for the Aziz–Slaman[14] and Aziz–Slaman[14]+Axilrod–Teller[5] intermolecular potentials. Miyano[29] has also reported some calculations for argon using the BFW potential. The comparison with experiment in Fig. 1 indicates that both the BFW and Aziz–Slaman potentials do not predict the liquid phase coexisting density of argon adequately. There is generally fair agreement for the vapor-branch of the coexistence curve. This contrasts with calculations using the Lennard-Jones potentials which normally yields good agreement with experiment for liquid densities. The good agreement often reported[9] with the Lennard-Jones potential is fortuitous and probably arises for the ''effective'' many-body nature of the potential. It is apparent from Fig. 1 that genuine two-body potentials cannot predict the liquid-phase densities of argon adequately. The results obtained from the BFW and Aziz–Slaman potentials are almost identical.

Anta *et al.*[10] reported that the addition of the Axilrod–Teller term to the Aziz–Slaman potential resulted in a considerable improvement in the agreement between theory and experiment as is illustrated in Fig. 1. Figure 1 also shows that the addition of the three-body term to the BFW potential results in good overall agreement of theory with experimental data. The average relative deviations for the vapor and liquid densities are 36.4% and 2.3%, respectively.

The contributions to both pressure and configurational energy of the various multipole terms to the three-body interactions of argon are identified in Table II. The contribution of three-body interactions to the vapor phase is negligible whereas they make an important contribution to the liquid-phase. The various three-body contributions to the configurational energy of the liquid-phase of argon are compared graphically in Fig. 2. Although Anta *et al.*[10] reported values of density, temperature, pressure, and configurational energies they did not report the contribution of three-body interactions to either the pressure or energy. It is evident from both the data in Table II and the comparison in Fig. 2 that the triple-dipole term makes the dominant contribution

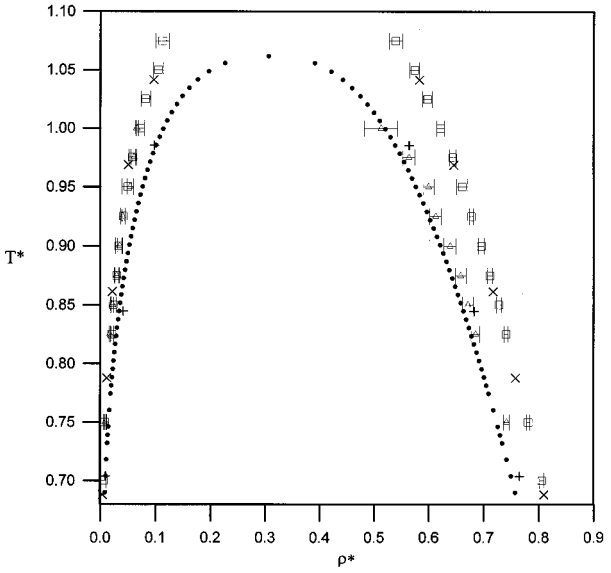

FIG. 1. Comparison of experiment (●, Ref. 32) with calculation using the BFW potential [Eq. (1)] (□), the Aziz–Slaman potential (×, Ref. 10), the Aziz–Slaman+Axilrod–Teller (+, Ref. 10) and the BFW+three-body (DDD+DDQ+DQQ+QQQ+DDD4) potentials (△) for the vapor–liquid coexistence of argon.

to three-body interactions. The other third-order multipole interactions ($u_{DDQ}+u_{DQQ}+u_{QQQ}$) contribute approximately 32% of the triple-dipole term. However, the effect of this contribution is offset largely by an approximately equal contribution (26% of the triple-dipole term) from fourth-order triple-dipole interactions of opposite sign. Consequently, the Axilrod–Teller term alone is an excellent approximation of three-body dispersion interaction. This conclusion is consistent with earlier work[7] on the relative magnitude of three-body interactions.

To the best of our knowledge, previous work on the effect of three-body interactions on the phase behavior of fluids has been confined exclusively to argon. In Tables IV–VII we report calculations for the vapor–liquid coexistence of krypton and xenon. The coexistence properties calculated from two-body potentials are summarized in Tables IV (krypton) and VI (xenon) whereas calculations including two-body and three-body terms are found in Tables V (krypton) and VII (xenon). The krypton and xenon atoms are considerably larger than argon and it can be anticipated that their increased polarizability may result in an increase in the relative importance of three-body interactions. The comparison of experiment with theory for the vapor–liquid coexistence of krypton and xenon is illustrated in Figs. 3 and 4, respectively. For both krypton and xenon, the two-body potentials

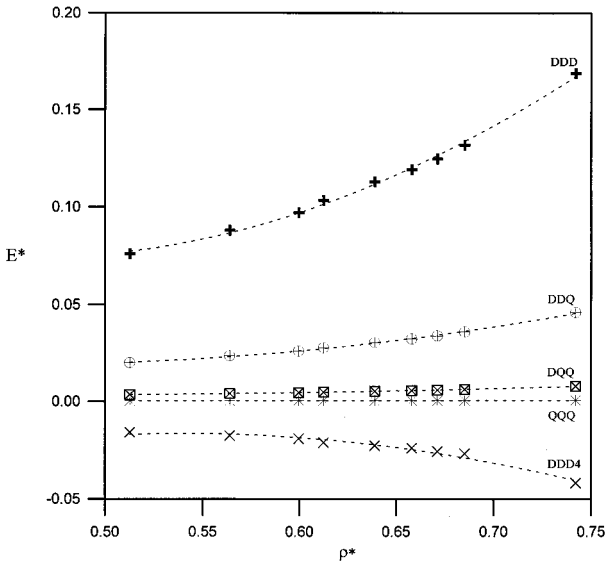

FIG. 2. Comparison of the contribution of the various three-body terms to the configurational energy of the liquid-phase of argon.

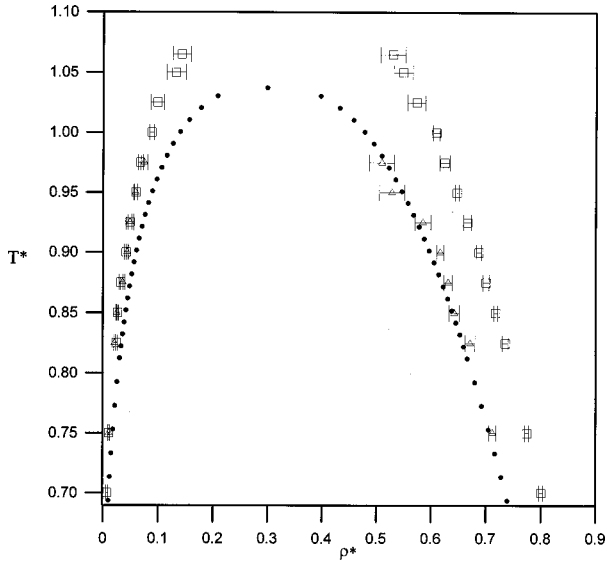

FIG. 3. Comparison of experiment (●, Ref. 32) with calculation using the two-body potential of Barker *et al.* [Eq. (3)] (□) and the Barker *et al.* [Eq. (3)]+three-body (DDD+DDQ+DQQ+QQQ+DDD4) potentials (△) for the vapor–liquid coexistence of krypton.

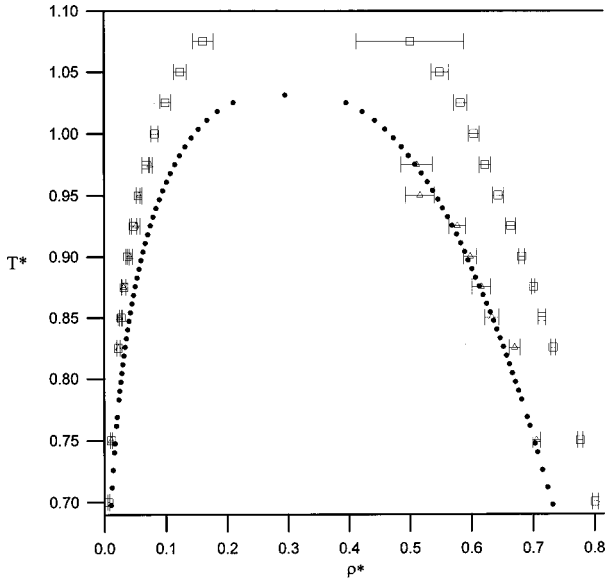

FIG. 4. Comparison of experiment (●, Ref. 32) with calculation using the two-body potential of Barker *et al.* [Eq. (3)] (□) and the Barker *et al.* [Eq. (3)]+three-body (DDD+DDQ+DQQ+QQQ+DDD4) potentials (△) for the vapor–liquid coexistence of xenon.

fail to represent the liquid-phase densities adequately whereas there is generally fair agreement for the vapor phase. However, it is evident that the addition of three-body interactions results in very good agreement of theory with experiment for subcritical liquid-phase densities. For krypton, the average relative deviations for the vapor and liquid densities are 34.5% and 1.9%, respectively. For xenon, the average relative deviations for the vapor and liquid densities are 35.8% and 1.4%, respectively. It should be stressed that in all cases the agreement between theory and experiment represent genuine predictions and no attempt has been made to optimize the agreement by altering the intermolecular potential parameters.

The relative contribution of the various multipole terms (Tables V and VII) to the three-body interactions of krypton and xenon is similar to the conclusions reached for argon. Interestingly, for xenon, the magnitude of the contribution from the fourth-order triple-dipole term is actually slightly greater than the dipole–dipole–quadrupole, dipole–quadrupole–quadrupole, and triple-quadrupole terms combined. Therefore, for krypton and xenon, the Axilrod–Teller term alone is a good representation of three-body interactions because the contribution of other multipole terms is offset by the contribution from the fourth-order triple-dipole term.

This work has not considered the possibility of interactions from three-body repulsion. There is evidence[1,9] that suggests that three-body repulsion may offset the contribution of Axilrod–Teller interactions by as much as 45%. However, this conclusion is based largely on approximate models[30] of three-body repulsion that are tied closely the Lennard-Jones potential. The lack of theoretical insight into three-body repulsion is in contrast to the well-developed models of three-body dispersion. It has been suggested[31] that three-body repulsion may improve the prediction of the thermodynamic properties of xenon. However, the good results obtained for argon, krypton, and xenon without including three-body repulsion, may indicate that three-body repulsion does not contribute significantly to vapor–liquid coexistence.

IV. CONCLUSIONS

We have demonstrated that three-body dispersion interactions have a significant effect on the vapor–liquid transition of argon, krypton, and xenon. The addition of three-body dispersion terms to an accurate two-body potential, results in good overall agreement of theory with experimental data. The Axilrod–Teller term alone is an excellent representation of three-body dispersion interactions because the effects of other third-order multipole terms are offset substantially by fourth-order triple-dipole interactions.

ACKNOWLEDGMENTS

We thank Dr. M. Lombardero for providing numerical values of the simulation data for the Aziz–Slaman potential reported graphically in Ref. 10. GM thanks the Australian government for an International Postgraduate Research Award (IPRA). Generous allocations of computer time on the Fujitsu VPP300 and NEC SX-4/32 computers were provided by the Australian National University Supercomputer Centre and the CSIRO High Performance Computing and Communications Centre, respectively.

[1] G. C. Maitland, M. Rigby, E. B. Smith, and W. A. Wakeham, *Intermolecular Forces, Their Origin and Determination* (Clarendon, Oxford, 1981).
[2] J. A. Barker, R. A. Fisher, and R. O. Watts, Mol. Phys. **21**, 657 (1971).
[3] A. Monson, M. Rigby, and W. A. Steele, Mol. Phys. **49**, 893 (1983).
[4] M. J. Elrod and R. J. Saykally, Chem. Rev. **94**, 1975 (1994).
[5] B. M. Axilrod and E. Teller, J. Chem. Phys. **11**, 299 (1943).
[6] R. J. Bell, J. Phys. B **3**, 751 (1971).
[7] M. B. Doran and I. J. Zucker, J. Phys. C **4**, 307 (1971).
[8] A. Z. Panagiotopoulos, N. Quirke, M. Stapleton, and D. J. Tildesley, Mol. Phys. **63**, 527 (1988).
[9] R. J. Sadus and J. M. Prausnitz, J. Chem. Phys. **104**, 4784 (1996).
[10] J. A. Anta, E. Lomba, and M. Lombardero, Phys. Rev. E **55**, 2707 (1997).
[11] R. J. Sadus, Fluid Phase Equilibria **144**, 351 (1998).
[12] R. J. Sadus, Fluid Phase Equilibria **150–151**, 63 (1998).
[13] R. J. Sadus, Ind. Eng. Chem. Res. **37**, 2977 (1998).
[14] R. A. Aziz and M. J. Slaman, Mol. Phys. **58**, 679 (1986).
[15] J. A. Barker and A. Pompe, Aust. J. Chem. **21**, 1683 (1968).
[16] M. V. Bobetic and J. A. Barker, Phys. Rev. B **2**, 4169 (1970).
[17] J. A. Barker, R. O. Watts, J. K. Lee, T. P. Schafer, and Y. T. Lee, J. Phys. Chem. **61**, 3081 (1974).
[18] R. J. Sadus, *Molecular Simulation of Fluids: Theory, Algorithms, and Object-Orientation* (Elsevier, Amsterdam, 1999).
[19] B. M. Axilrod, J. Chem. Phys. **19**, 719 (1951).
[20] P. J. Leonard and J. A. Barker, in *Theoretical Chemistry: Advances and Perspectives*, edited by H. Eyring and D. Henderson (Academic, London, 1975), Vol. 1.
[21] W. L. Bade, J. Chem. Phys. **28**, 282 (1958).
[22] M. A. van der Hoef and P. A. Madden, Mol. Phys. **94**, 417 (1998).
[23] M. P. Allen and D. J. Tildesley, *Computer Simulation of Liquids* (Clarendon, Oxford, 1987).
[24] P. Attard, Phys. Rev. A **45**, 5649 (1992).
[25] R. A. Aziz, A. R. Janzen, and M. R. Moldover, Phys. Rev. Lett. **74**, 1586 (1995).
[26] E. Ermakova, J. Solca, G. Steinebrunner, and H. Huber, Chem.-Eur. J. **4**, 377 (1998).
[27] B. Kirchner, E. Ermakova, J. Solca, and H. Huber, Chem.-Eur. J. **4**, 383 (1998).
[28] B. Smit, Ph. De Smedt, and D. Frenkel, Mol. Phys. **68**, 931 (1989).
[29] Y. Miyano, Fluid Phase Equilibria **95**, 31 (1994).
[30] A. E. Sherwood and J. M. Prausnitz, J. Chem. Phys. **41**, 429 (1964).
[31] E. Rittger, Mol. Phys. **71**, 79 (1990).
[32] N. B. Vargaftik, *Handbook of Physical Properties of Liquids and Gases* (Hemisphere, Washington, DC, 1975).